

Crystal 3D Analysis in Micrographs Applied to Cellular COVID Anomalies Identification

Bolivia Cuevas-Otahola¹, Jesús Arriaga-Hernandez²,
María Morín-Castillo¹, José Oliveros-Oliveros²,
Ana Vega-Salgado³

¹ Benemérita Universidad Autónoma de Puebla,
Facultad de Ciencias de la Electrónica,
Mexico

² Benemérita Universidad Autónoma de Puebla,
Facultad de Ciencias Físico Matemáticas,
Mexico

³ Instituto Nacional de Astrofísica,
Departamento de Óptica,
Mexico

{bolivia.cuevasotahola, jesus.arriagahernandez}@viep.com.mx,
maria.morin@correo.buap.mx, oliveros@fcfm.buap.mx,
karem.vega@inaoe.mx

Abstract. In this work, we introduce a set of algorithms, constituting an image processing technique based on algebraic-topological and probabilistic concepts, to carry out 3D objects recognition in flat images (FI) with flat illumination and perpendicular to the objects plane. Such features are found in micrographs from SEM (Scanning Electron Microscope), TEM (Transmission Electron Microscope), and HIM (Helium Ion Microscopy). Hence, our work is based on the analysis of FI obtained by HIM to observe the COVID-19 behavior in controlled cell cultures. We found a certain optimization in the characterization of anomalies due to COVID-19 for cell cultures Vero E6, infected with COVID-19, allowing us to determine if the COVID-19 overlaps or joins (as a cell anomaly deforming a given zone) the cell membrane.

Keywords: Image processing, helium ion microscopy (HIM), 3d objects recognition, COVID-19 cell behavior, cell culture anomalies.

1 Introduction

In this work, we obtain 3D objects from FI obtained by HIM for Vero 6 cells infected with COVID-19, obtained and analyzed with a medical scope by Frese et al. [6]. To this aim, we set as a base the algorithms developed by Arriaga et al. [4, 3], Gerchberg-Saxton [7] modified with the 2D Legendre polynomials [2] based on the concepts to build the isomorphism in Arriaga et al. [1], to identify and analyze anomalies as a source of cell pathologies from their GT.

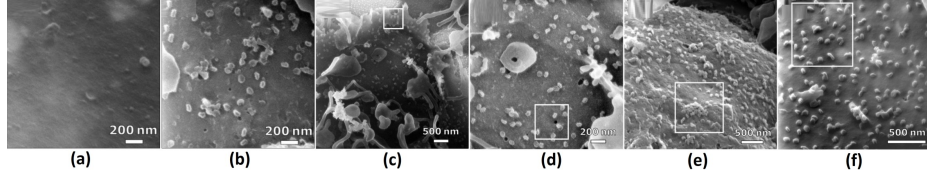


Fig. 1. In (a), we show mock-infected cells with FOV $1.7 \mu\text{m}$, in (b) MOI-1 with FOV $1.7 \mu\text{m}$, in (c) MOI-1 at FOV $5 \mu\text{m}$, and in (d) FOV at $2 \mu\text{m}$, without charge compensation in (e) and (f) MOI-1 with charge compensation with FOV $3.5 \mu\text{m}$, and $2 \mu\text{m}$.

We have developed these techniques to segment images using the GT histogram and filter using binary masks [8]. On the other hand, we developed the Gercberg-Saxton with the 2D Legendre polynomials [4] to recover the information and reduce the image noise. We increase the image resolution creating intermediate points between the original image pixels by interpolating in terms of the 1D Legendre polynomials in probabilistic regimes [2], allowing us to observe anomalies leading us to the identification of pathologic sources.

1.1 Main Applied Techniques

We use an isomorphism based on the GT images analysis, with flat illumination perpendicular to the analyzed object (see Arriaga et al. [1]), with a base \hat{e}_1 (pixel 1) and \hat{e}_0 (pixel 0) in a linear combination $P_{i,j} = \alpha_{i,j} \hat{e}_1 + \beta_{i,j} \hat{e}_0$, with $\alpha_{i,j}$ and $\beta_{i,j}$ scalars in \mathbb{R} , and i, j , denoting the matrix entries, rows and columns, respectively.

We obtain the vector space V_{RM} . We re-scale the GT in $l = \{l_i \mid i \in [0, 255] \subset \mathbb{Z}\}$ to $g = \{g_j \mid \{j \in [1, 256] \subset \mathbb{Z}\} \cup 0\}$, associating the white color to the tone g_{256} , and black with g_1 . Hence, the FI image is given by $\{\hat{e}_0, \hat{e}_1\}$, generating the FI with $\vec{K}_{i,j} = \gamma_{i,j} \hat{e}_1 + \eta_{i,j} \hat{e}_0$, with $\gamma_{i,j}$ and $\eta_{i,j}$ scalars in $[1, 256] \subset \mathbb{Z} \subset \mathbb{R}$. The latter results in $(\{\hat{e}_0, \hat{e}_1\})$ for the vectors spaces V_{RM} , and V_{PI} , where the space V_{RM} is built from the space V_{PI} , defining an isomorphism [1]. Hence, we define:

Let V_{RM} the vector space defined as the RM images, V_{FI} the vector space defining the FIs and the metric d (a real function). If for two vectors from different pixels and gray tones holds $d(\vec{K}_{l,h}, \vec{K}_{i,j}) = 0$, then, for the pixels in which g reaches a minimum difference holds $T(K_{i,j}) = P_{i,j}$, and $T(K_{l,h}) = P_{l,h}$ simultaneously.

Here $d(.,.)$ is a metric function, representing, in this case, the distance between different GT vectors regarding the previously mentioned base, and T is a linear mapping. We modify the Gerchberg-Saxton algorithm with the 2D Legendre polynomials [4], considering the algorithm by Gerchberg et al. [7], where a numerical Fourier transform (FFT) is used to reduce noise and recover the phase.

We optimize the iterative process before applying the inverse transform (IFFT), performing a low-order multilinear fit based on the 2D Legendre polynomials in Arriaga et al. [4]. Finally, we use the 1D Legendre polynomials (LP) as a base capable of generating any family of polynomials based on the LP from a linear regression.

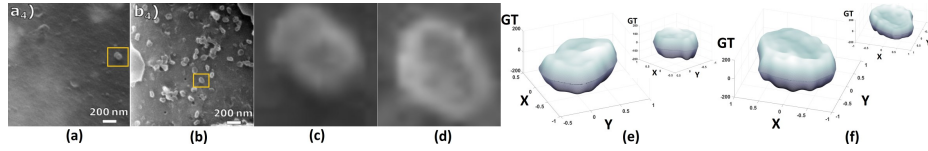


Fig. 2. In (a) and (b), we show a simple segmentation, in (c) and (d) the Gerchberg-Saxton algorithm [7] application, modified with the 2D-LP [2], and in (e) and (f) the 3D objects applying the isomorphism in Arriaga et al. [1].

We build the most probable pixels between the existing pixels, using linear fits, interpolations, and regressions (Arriaga et al. [2]), generating an image with a higher resolution, having the most probable information according to that of the original image, based in probabilistic theory and linear algebra.

1.2 Image Selection and Segmentation

The HIM (Helium ion microscopy) image analysis, is characterized by the obtained sub-nanoscale range images [6], in cell biology [5], stem cells [10], and with less impact in the analysis of biological samples. The HIM application to visualize viruses and hosts has been used in the analysis of *E. coli* bacteria infected with Fago T4 [9], etc.

We obtain medical images of Vero E6 cells infected with COVID-19 from the work by Frese et al. [6], using an innovative technique in the area of HIM (Helium ion Microscopy). We focused on the results shown in Fig. 1 with size 1024×1024 for a Vero E6 analysis, biologically mock-infected and infected at MOI (multiplicity of infection) of approximately 1 (MOI 1).

In Fig. 1 (a), we show mock-infected cells with FOV (field of view) of $1.7 \mu\text{m}$, in Fig. 1 (b) MOI-1 infected cells with FOV of $1.7 \mu\text{m}$. We show the results by Frese [6] with the effects of the deposited carbon over the samples during the images formation with the HIM. However, due to the involved charge conductivity, the study region looks brighter, showing an infected cell in MOI-1 at a FOV of $5 \mu\text{m}$ in Fig. 1 (c).

Subsequently, we move over the cell culture plane to obtain an image with a FOV of $2 \mu\text{m}$ in Fig. 1 (d), in both cases without compensating the charge. Finally, we obtain cell culture images of the infected cells in MOI-1 with charge compensation with FOV $3.5 \mu\text{m}$ in Fig. 1 (e), showing, subsequently, a different sample with FOV $2 \mu\text{m}$.

2 Results

In the first place, we focus on the interest zones in each image (Fig. 1) to carry out a preliminary segmentation procedure, highlighting the objectives of the base work, analyzing the cell cultures with COVID-19, where we observe cell anomalies joined to the membrane and just overlapped.

Hence, in Fig. 2 (a) and (b), we show a simple segmentation procedure with a square region (similar to the original one in Frese, in their Figs. 1 (a) and (b), to show the extent of our processing techniques). Subsequently, we apply the i-LP by Arriaga et al. [2] to increase the image resolution from 100×100 to 700×700 pixels with a mean error margin of 0.037% regarding the zoom-in performed by Frese [6].

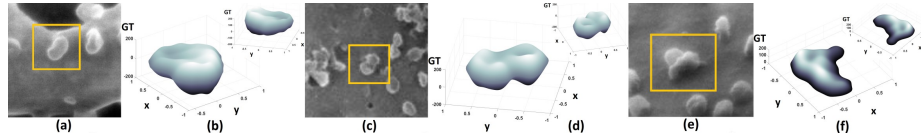


Fig. 3. In (a), (c) and (e), we show the i-LP (Arriaga et al. [2]) application, the Gerchberg-Saxton [7] modified in Arriaga et al. [4] and the isomorphism by Arriaga et al. [1], to obtain an object with a 3D relief, with a resolution of 1024×1024 pixels in (b), (d), and (f).

In Fig. 2 (c) and (d), we show the Gerchberg-Saxton algorithm application [7] modified with the 2D-LP [2], with a low-order in each iteration (degrees 3, 4, 5 and 6 of the 2D Legendre polynomials) [4], and in Figs. 2 (e) and (f), we show normalized images (in GT with magnitudes up to 1) of the application of the isomorphism in Arriaga et al. [1] to obtain the 3D profile (as a 3D object in Matlab ®) and, in the upper panel, we include an image rotation.

The heights identified by the isomorphism are an approximation to the 3D objects from the image GT, highly depending on the technique (HIM, SEM, or TEM), due to the illumination, and image scale, since from a longitudinal measurement, the GT is interpreted to provide an approximate height value. We analyze the images in Figs. 1 (b), (c), (f) of the results by Frese et al. [6] to apply the simple segmentation procedure and a more complex one by polygons or histograms in GT to segment particles and cells contaminated by COVID-19.

In Fig. 3, we apply i-LP by Arriaga et al. [2] to segment the images in Figs. 1 (c), (b), (f), respectively, and subsequently applied the Gerchberg-Saxton [7] modified with the 3th-degree 2D Legendre polynomials, as shown in Arriaga et al. [4]. As the following step, we apply the isomorphism by Arriaga et al. [1] to obtain an object as a 3D relief as we show in Figs. 3 (b), (d) and (f).

We highlight the objective of identifying the coupling or contamination due to COVID-19 in the cell culture in Figs. 3 (b) and (d), observing a superposition. However, in the case in Fig. 3 (f), we show more advanced contamination, where the COVID-19 is completely attached to the cell membrane, being an anomaly yet to be studied to determine the extent in the affected organism from its cellular structure.

3 Conclusions

In this work, we consider a set of techniques we have developed in medical image processing [8] with mathematical bases for the identification of sources as cell anomalies. Such techniques are the i-LP by Arriaga et al. [2], the Gerchberg-Saxton modified with the 2D Legendre polynomials by Arriaga et al. [4] and the isomorphism by Arriaga et al. [1], with the aim of segmenting, increasing the resolution, reducing noise and recovering the phase, obtaining 3D profiles of objects in flat images.

The main objective was recovering the 3D profiles, subsequently accomplished in Figs. 2 and 3, and sharing the objective in Frese et al. [6], we can determine if the COVID-19 particles are overlapped to the cell culture or represent a cell anomaly by deforming, feeding, consuming, mutating, and modifying the cell membrane. We resolve the latter in the objects in Figs. 3 (b), (d) and (f).

Acknowledgments. The authors want to thank Benemérita Universidad Autónoma de Puebla (BUAP) for the support given during this research work. We also thank CONACYT (Consejo Nacional de Ciencia y Tecnología, México).

References

1. Arriaga-Hernández, J., Cuevas-Otahola, B., Jaramillo-Núñez, A., Oliveros-Oliveros, J., Morín-Castillo, M.: Optical-topological concepts in isomorphisms projecting bi-Ronchi masks to obtain 3D profiles from objects in 2d images. *Applied Optics*, vol. 59, no. 33, pp. 10464–10473 (2020) doi: 10.1364/AO.401316
2. Arriaga-Hernández, J., Cuevas-Otahola, B., Oliveros-Oliveros, J., Morín-Castillo, M.: Two-dimensional legendre polynomials as a basis for interpolation of data to optimize the solution of the irradiance transport equation analyzed as a boundary problem on surfaces testing. *Applied Optics*, vol. 58, no. 18, pp. 5057–5066 (2019) doi: 10.1364/AO.58.005057
3. Arriaga-Hernández, J., Cuevas-Otahola, B., Oliveros-Oliveros, J., Morín-Castillo, M.: Geometric aberrations in the 3D profile of microparticles observed in optical trapping using 2D legendre polynomials. *Optik*, vol. 23, no. 12, pp. 1–25 (2021) doi: 10.1016/j.ijleo.2021.168123
4. Arriaga-Hernández, J. A., Cuevas-Otahola, B., Oliveros-Oliveros, J., Morín-Castillo, M.: 3D mapping in optical trapping of polystyrene particles applying the Gerchberg-Saxton modified with 2D legendre polynomials. *Journal of Optics*, vol. 23, no. 12, pp. 1–11 (2021) doi: 10.1088/2040-8986/ac303c
5. Bazou, D., Behan, G., Reid, C., Boland, J. J., Zhang, H. Z.: Imaging of human colon cancer cells using He-Ion scanning microscopy. *Journal of Microscopy*, vol. 242, no. 3, pp. 290–294 (2011) doi: 10.1111/j.1365-2818.2010.03467.x
6. Frese, N., Schmerer, P., Wortmann, M., Schörmann, M., König, M., Westphal, M., Weber, F., Sudhoff, H., Götzhäuser, A.: Imaging of SARS-CoV-2 infected vero E6 cells by helium ion microscopy. *Beilstein Journal of Nanotechnology*, vol. 12, no. 13, pp. 172–179 (2021) doi: 10.3762/bjnano.12.13
7. Gerchberg, R. W., Saxton, W. O.: A practical algorithm for the determination of the phase from image and diffraction plane pictures. *Optik*, vol. 35, no. 2, pp. 237–246 (1972)
8. Jaramillo-Núñez, A., Arriaga-Hernández, J., Cuevas-Otahola, B., Pérez-Meza, M., Sánchez-Rinza, B.: Diagnostic software proposal for bone scan follow-up using false color based on the gammagrams analysis from gray tone histograms. *Biomedical Physics and Engineering Express*, vol. 7, no. 3, pp. 1–11 (2021) doi: 10.1088/2057-1976/abe680
9. Leppänen, M., Sundberg, L. R., Laanto, E., de Freitas-Almeida, G., Papponen, P., Maasilta, I. J.: Imaging bacterial colonies and phage–bacterium interaction at sub-nanometer resolution using helium-ion microscopy. *Advanced Biosystems*, vol. 1, no. 8, pp. 1700070 (2017) doi: 10.1002/adbi.201700070
10. Schürmann, M., Frese, N., Beyer, A., Heimann, P., Widera, D., Mönkemöller, V., Huser, T., Kaltschmidt, B., Kaltschmidt, C., Götzhäuser, A.: Helium ion microscopy visualizes lipid nanodomains in mammalian cells. *Small*, vol. 11, no. 43, pp. 5781–5789 (2015) doi: 10.1002/sml.201501540